THE INFLUENCE OF A HYDRIDED LAYER ON THE FRACTURE OF ZIRCALOY-4 CLADDING TUBES*

Robert S. Daum
Argonne National Laboratory, Argonne, IL 60439

Douglas W. Bates[1], Donald A. Koss and Arthur T. Motta
The Pennsylvania State University, University Park, PA 16802
([1]Currently with U.S. Navy)

April 2002

* Submitted to the International Conference on Hydrogen Effects on Material Behavior and Corrosion Deformation Interactions, Moran, WY, September 22-27, 2002.

Work supported by U.S. Nuclear Regulatory Commission, Office of Nuclear Regulatory Research.

THE INFLUENCE OF A HYDRIDED LAYER ON THE FRACTURE OF ZIRCALOY-4 CLADDING TUBES

Robert S. Daum
Argonne National Laboratory, Argonne, IL 60439

Douglas W. Bates[1], Donald A. Koss and Arthur T. Motta
The Pennsylvania State University, University Park, PA 16802

Abstract

During operation of nuclear power reactors, irradiated Zircaloy™-4 cladding tubes contain circumferentially oriented hydrides concentrated in a layer near the outer surface of the cladding. This study has investigated the effect of a hydride layer or "rim" located near the outer surface of the cladding tube on the failure of *unirradiated* Zircaloy-4 cladding tubes. Utilizing plane-strain ring-stretch tests with the maximum principal stress along the circumferential or hoop direction, we examined the influence of a hydride rim on the failure of unirradiated Zircaloy-4 cladding at both room temperature and 300°C. Fracture is found to be sensitive to hydride-rim thickness such that cladding tubes with a hydride-rim thickness >140 μm (≈700 wppm total hydrogen) exhibit brittle behavior, while cladding tubes with a rim thickness <90 μm (≈600 wppm) remains ductile. The mechanism of failure is identified as strain-induced micro-crack initiation within the hydride rim, linkage of micro-cracks to form a long crack, and subsequent failure within the uncracked ligament due to either a shear instability or ductile crack growth. The increased ductility of cladding with small hydride-rim thicknesses appears to be related to the linkage of short cracks into a long surface crack.

Introduction

The mechanical behavior of the zirconium-based nuclear fuel cladding degrades during steady-state operation in light water reactors due to a combination of oxidation, hydriding, and radiation damage. In an effort to decrease operating costs of these reactors through the use of longer fuel cycles, and to reduce the volume of waste associated with core reloads, utilities have a strong incentive to extend the use of fuel assemblies to higher burnup levels. Further increases in operating efficiency of power reactors can also be achieved by increasing the coolant outlet temperature. Both of these operating procedures enhance cladding degradation, which may increase the likelihood of cladding failure during design-basis accidents.

Losses of cladding ductility at high levels of fuel burnup are believed to result from a combination of three effects: radiation damage, oxidation, and hydriding [*1-3*]. Radiation damage from fast neutrons increases the dislocation density in recrystallized material causing hardening. However, this increase in dislocation loop density is thought to saturate at relatively low exposures [*2*]. During service, the cladding undergoes oxidation with associated hydrogen pickup; the total amount of hydrogen increases steadily with fuel burnup [*4*] and, once the terminal solubility is exceeded, hydride precipitates form. Owing to cladding texture and thermal gradients, the hydride formation in irradiated zirconium-based cladding tubes consists of circumferentially oriented hydrides concentrated in a layer or "rim" near the outer surface of the cladding. Thus, in irradiated cladding, a hydride rim often resides above a substrate that is

[1]Currently with U.S. Navy
Zircaloy™ is a trademark of Westinghouse Electric Corporation

relatively free of hydrides. Given the texture in the Zircaloy-4 cladding tubes used in light water reactors, the hydride layer consists of aligned, circumferentially-oriented hydride platelets [*5-7*]. A prediction of the ductility of such cladding must take the following into account: the presence of the hydrides as a layer/rim and the rim thickness, the ability of the hydrides to deform [*6-9*], their circumferential orientation within the hydrided layer, and the presence of a relatively unhydrided substrate.

A second condition that affects the sensitivity of high burnup cladding to hydrogen is the stress state. It is well known that elevating the level of the stress triaxiality ratio decreases the fracture strain of recrystallized zirconium alloy sheet containing uniform distributions of hydrides [*8,10*]. In the case of Cold-Worked and Stress-Relieved (CWSR) Zirconium alloy cladding tubes subject to postulated reactor accidents such as the reactivity-initated accident (RIA), the interaction between the fuel pellet and the cladding tube forces the cladding to deform under multi-axial tensile stress states; these are generally believed to be in the range $1 \leq (\sigma_\theta/\sigma_z) \leq 2$, where σ_θ is the hoop stress component and σ_z is the axial stress component. In other words, the cladding tube is forced to deform under stress states ranging between equal-biaxial tension ($\sigma_\theta/\sigma_z = 1$) and transverse plane-strain tension ($\sigma_\theta/\sigma_z = 2$ for a plastically isotropic tube). To address this stress-state issue, we have recently developed a "transverse, plane-strain, ring-stretch tension test" [*11,12*]. That test utilizes a double-edge notched ring specimen in which the notches impose a near plane-strain deformation path within the specimen. Owing to the plastic anisotropy of the Zircaloy cladding ($R = 2.3$ for unirradiated Zircaloy-4 tubing, where R = width-strain/thickness-strain in uniaxial hoop tension [*11*]), a plane-strain deformation path imposes multi-axial tension such that $(\sigma_\theta/\sigma_z) \cong 1.4$, or within the range of multiaxial stress states imposed during a postulated RIA.

While the influence of a *uniform* distribution of hydrides on the tensile ductility of zirconium-based alloys has been studied extensively [*8-10,13,14*], failure behavior when hydrides are non-uniformly distributed in the form of a layer or rim has not been thoroughly addressed. A few studies [*9,15-17*] have observed an effect of a hydride rim on hoop ductility of unirradiated cladding tubes. In particular, *Kitano* [*16*] has shown a significant reduction in unirradiated cladding strains for hydride rim thicknesses of >95 μm and >110 μm under uniaxial and biaxial hoop tension, respectively. These results suggest that a ductile-to-brittle transition occurs in the deformation behavior of cladding tubes containing a a finite hydride rim thickness.

Additionally, previous studies [*18,19*] have investigated the effect of a hydride rim on the failure path of Zircaloy-4 cladding tubes irradiated to high fuel burnups and subjected to RIA-simulation tests. Although not quantitative, according to post-test examinations, *Garde* and *co-workers* [*18*] and *Fuketa* and *co-workers* [*19*] suggest that fracture initiation occurs in the hydride rim by brittle crack growth and, depending on temperature and loading path, followed by either ductile or brittle fracture of the remaining cladding ligament.

The purpose of this study is to explore the response of unirradiated Zircaloy-4 cladding tubes that contain hydrides concentrated in the form of a thin layer near the outer surface, as is typical of high-burnup cladding [*19*]. Using "ring-stretch" specimen geometries in order to impose multi-axial stresses and near plane-strain tension in the hoop direction of the cladding tube, we examine the influence of thin layers of hydrides on the ductility of Zircaloy-4 cladding subject to stress states relevant to potential in-service accidents such as the RIA.

Experimental Procedures

Material

As in previous studies [*12,15,17*], Zircaloy-4 cladding tubes were obtained from Sandvik Metals and Westinghouse Electric Corporation in a CWSR condition with outer diameter of

approximately 9.5 mm and wall thicknesses of approximately 0.56 mm. The grain structure consists of elongated grains with ≈10:1 aspect ratio, oriented parallel to the tube axis and ≈10-15 μm long and ≈1-2 μm thick. As-fabricated Zircaloy-4 possesses a crystallographic texture in which the basal planes tend to align with their basal poles inclined approximately ±40^{o} to the normal of the tube surface and oriented towards the tangential direction; the basal and prism pole intensities are up to ten times their random value.

In order to simulate the hydride distribution in high burnup cladding, unirradiated cladding tubes were artificially hydrided in an argon/hydrogen gas mixture at 327°C (600K) by M. Ozawa at Nuclear Development Corporation. The total hydrogen content was determined using an inert gas fusion technique. The total oxygen content of hydrogen-charged cladding was found to be approximately equal to that of as-fabricated cladding.

Figure 1 shows the microstructures consist of a relatively high concentration of circumferential hydrides concentrated primarily within a layer near the outer surface of the cladding tube, thus forming a "hydride rim". The thicknesses of the hydride rim varied from specimen to specimen and ranged from approximately 20 to 250 μm. In addition, a few hydrides exist within the "substrate" layer of the cladding tube below the hydride rim. It is significant that the hydride microstructure shown in Fig. 1 is similar to that observed in high-burnup fuel cladding [*19*].

To contrast the effect of a hydride rim on hoop tensile ductility, a few specimens that originally had hydride rims were machined to remove the hydride. The resulting microstructure consists of circumferential hydrides, but uniformly distributed through the thickness; the hydride rim was no longer present.

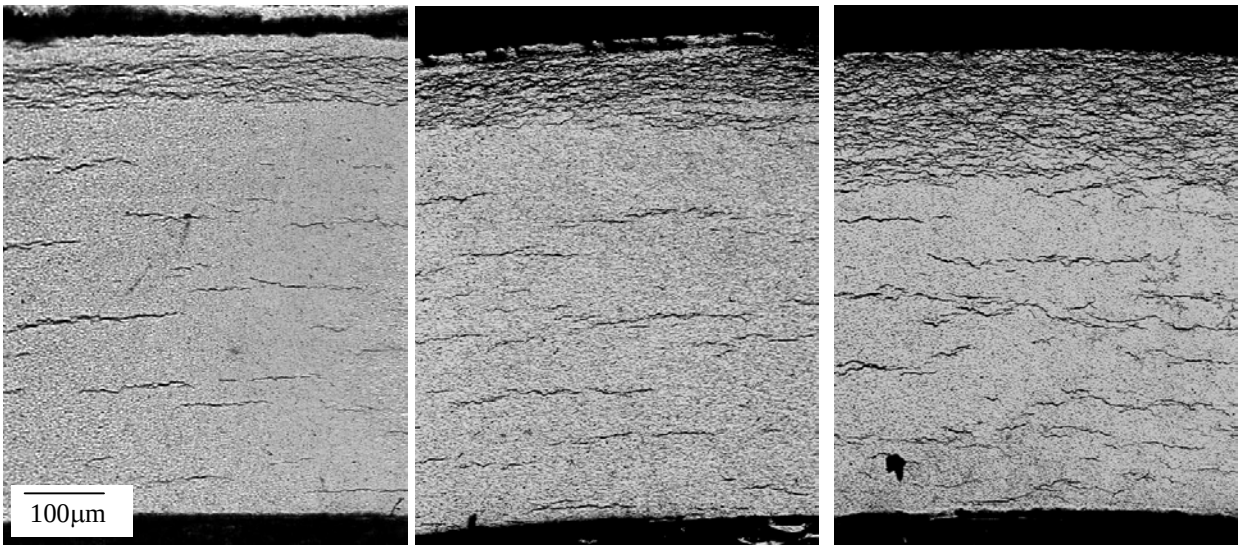

Figure 1: Light micrographs showing hydride microstructure and distribution within Zircaloy-4 cladding tubes with a hydride layer thicknesses of (a) 80, 100, and (c) 180 μm.

Mechanical Testing

In order to impose a biaxial stress state such that hoop extension of the cladding occurs by through-thickness slip, we used the double edge notched "transverse plane-strain ring-stretch" specimen shown in Fig. 2 and described in detail elsewhere [*11,12*]. The specimen uses the

constraints of the two notches to force the central region of the gauge section to deform such that there is little contraction across the specimen width (i.e., along the tube axis). As a result, a near plane-strain deformation condition is achieved, as has been supported by finite element modeling and by measurements of the local ratio of thickness to hoop strain **[***11***]**.

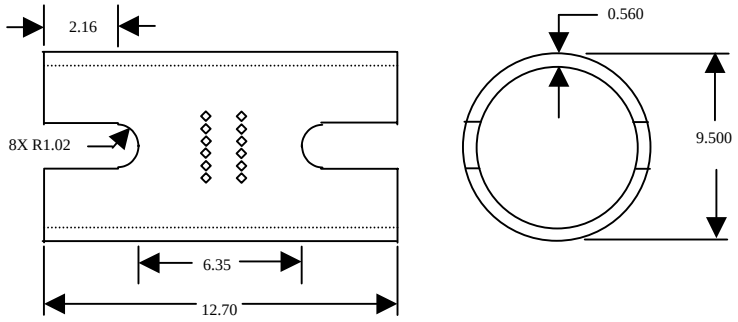

Figure 2: Plane-strain ring-stretch test specimen with micohardness indentation arrays for determining local strains (all dimensions are in mm and not-to-scale).

Also, as in previous studies [*11,12,15,17*], microhardness indentations were used to determine strains on a local basis along the specimen gauge length. This method has an accuracy of ± 0.01. Two measures of cladding failure were used. As described elsewhere [*11,12*], "limit strain" (ε_{limit}) is defined as the "uniform" deformation in the gauge section at material failure and is calculated by numerical integration from the as-measured strain distribution. Furthermore, the "fracture strain" (ε_{frac}) is defined as the local strain as determined over a 0.2 mm element containing the fracture surface. The tests were performed at an initial strain rate of $\approx 10^{-3}$/s, using loading fixtures consisting of two "D-shaped" die inserts that transmit the displacement to the specimen. In order to promote uniform deformation along the gauge section and limit effects of friction, a combination of Teflon™ tape and vacuum grease was used to lubricate the interface between the die inserts and the inner surface of the cladding specimen. Tests on un-irradiated/un-hydrided specimens using the above procedure confirm relatively uniform deformation along a gauge section somewhat greater than 2 mm long in the specimen shown in Fig. 2.

Results and Discussion

On the Failure Process

For cladding that has a dense layer of hydrides in the form of a rim near its outer surface, as shown in Fig. 1, our observations suggest the following failure process. Cracks initiate within the hydride rim upon yielding of the cladding tube, as are indicated in Fig. 3 (note that micro-cracks do not initiate at microhardness indents). Results from several specimens show that the crack density increases with decreasing hydride rim thickness such that only a few deep micro-cracks form within the cladding with thick hydride layers, while a high density of short micro-cracks form within the thin hydride layers. This crack density effect appears to be related to the presence of the free surface created by the crack flanks in inihibiting the initiation of neighboring cracks.

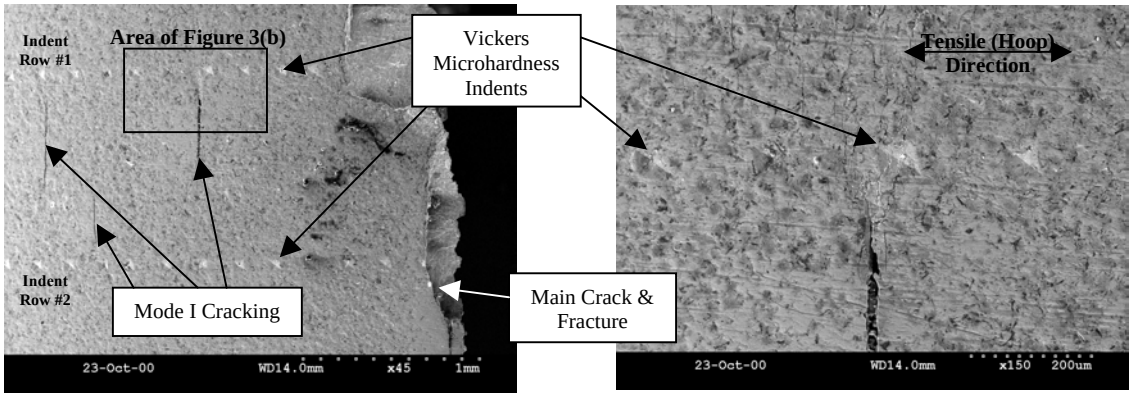

(a) (b)

Figure 3: Scanning electron micrographs at (a) low magnification and (b) higher magnification showing Mode I surface cracks initiating within a 148μm thick hydride rim after testing at room temperature.

The fracture path also differs in the thick-hydride rim and thin-hydride rim cladding. In *thin* hydride samples, the linking of multiple microcracks creates a long surface crack that, while not deep, is relatively planar. In this instance, strain accumulates while the short, microcracks, which are blunted in the relatively ductile substrate, link into a long, macrocrack that eventually propagates. As shown in Fig. 4, eventual fracture of the uncracked ligament occurs as a result of either damage-induced fracture (at room temperature; see Fig. 4a) or shear localization (at 300°C; see Fig. 4b). At room temperature, the damage-induced fracture occurs as the strain to nucleate, grow and coalesce voids (i.e., damage accumulation) is less than that required to develop a localized neck. The damage-accumulation fracture process will also be favored by an increased density of hydrides within the uncracked ligaments, such as might occur if the hydride layer is thick. In contrast, localized necking and shear failure of the uncracked ligament will likely be favored at 300°C where an increase in damage-induced fracture strain enables localization to develop [*11*].

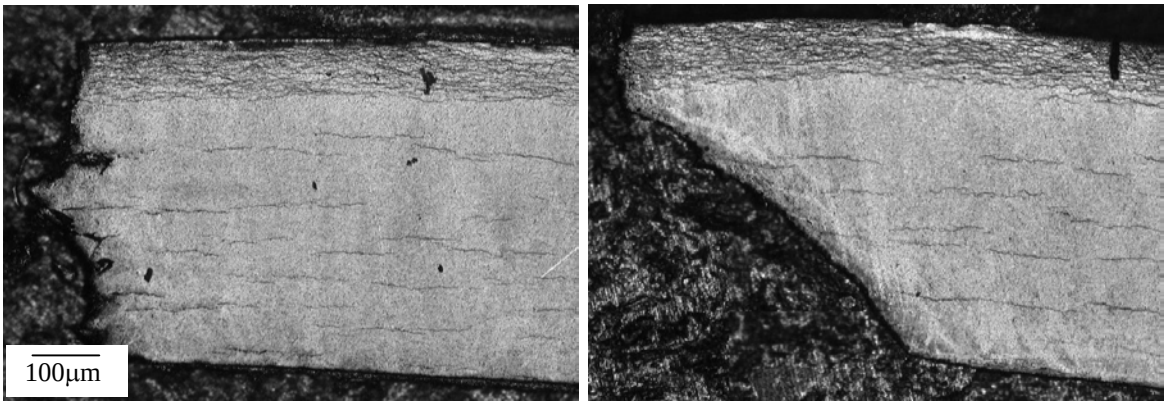

(a) (b)

Figure 4: Transverse fracture profiles of cladding with a hydride rim tested at (a) room temperature and (b) 300°C.

Previous studies [*18,19*] suggest a similar dependency of temperature on the fracture process of irradiated cladding. In particular, *Garde* and *co-workers* [*18*] found that, with increasing hydride dissolution in the ligament brought about by higher temperatures during an RIA, a transition from brittle crack growth to a more ductile fracture is predominant. Furthermore, these studies suggest that, regardless of testing temperatures during these RIA-simulation tests, fracture initiation occurred at the hydride rim on the outer surface of the tube as with out observations of unirradiated cladding.

Based on the above interpretation, we suggest that fracture of cladding with a hydride rim occurs by a multi-stage process, consisting of (1) initiation of short micro-cracks within the hydride rim, (2) growth and linkage of micro-cracks into a long surface crack, (3) cladding fracture due to the propagation of the long surface crack by either a damage accumulation process (room temperature failure) or failure of the relatively hydride-free ligament by shear instability (300°C failure). We discuss this in more detail below:

1. Initiation of micro-cracks. Our observations indicate that micro-cracks initiate at very small strains---essentially zero strain. Also, the density of micro-cracks initiated decreases with increasing hydride layer thickness as described above. Thus, thick hydride layers initiate a single deep crack, which propagates along its length extending across the entire specimen and resulting in near-brittle behavior.
2. When the hydride rim is thin, the growth and linkage of "shallow" micro-cracks into a long (surface) crack results in cladding ductility. This crack growth/linkage stage appears to depend on both the density of cracks *and* their depth. A high density of (relatively shallow) micro-cracks will link rather quickly with strain, forming a long but shallow surface crack. In contrast, a lower density of more widely spaced and non-coplanar surface cracks of intermediate depth link with difficulty. In this case, cladding ductility also occurs due to the strain-induced linking of moderately deep cracks into a tortuous long surface crack.
3. Failure of the cladding substrate below the hydride rim depends in a sensitive manner on rim depth, with strain to failure increasing as hydride-rim depth decreases. Crack growth in cladding with a thin hydride layer is relatively difficult and significant crack opening displacement occurs before growth due to damage accumulation at room temperature or shear instability at 300°C. Thus, cladding with thin hydride layers (i.e., 20 μm thick) forms a high density of shallow cracks that link easily but require significant strain to propagate in the form of a long surface crack. However, it appears that such cladding may show no more ductility than cladding with cracks of medium depth (i.e., ≈ 75 μm) *if* these cracks have difficulty linking. In the latter case, considerable strain is required to link distant, deep cracks (if they are not co-planar) and to propagate the subsequent long crack along a tortuous fracture path. Finally, in contrast, cladding with thick hydride layers will initiate a relatively deep crack that propagates easily as a deep, planar crack. Near-brittle behavior of the cladding results.

Effect of Hydride Layers on Ductility

Failure of the hydrided Zircaloy cladding was determined on the basis of strain distributions of failed specimens, as shown in Fig. 5a. It should be recognized that our strain values are based on elements initially 0.2 mm long. Thus, Fig. 5b indicates finite strain levels adjacent to crack over the 0.2 mm length scales even though we expect near zero strains immediately adjacent to the crack.

To determine ε_{limit},, the far-field strain at the failure, we recognize that, after cracks initiate within the hydrided rim, cladding hoop extension occurs before deformation

localization/fracture develops within the uncracked ligament. Therefore, the value of ε_{limit} includes the sum of the displacements accumulating during macro-crack formation and subsequent deformation in the uncracked ligaments but not those crack opening displacements associated with arrested micro-cracks and the macro-crack. Thus, Fig. 5b indicates a value of $\varepsilon_{limit} \cong 0.062$ as the level of strain present along the cladding tube at locations between cracks. The ε_{limit}-value may be viewed as a lower-limit cladding failure strain for unirradiated, hydrided cladding.

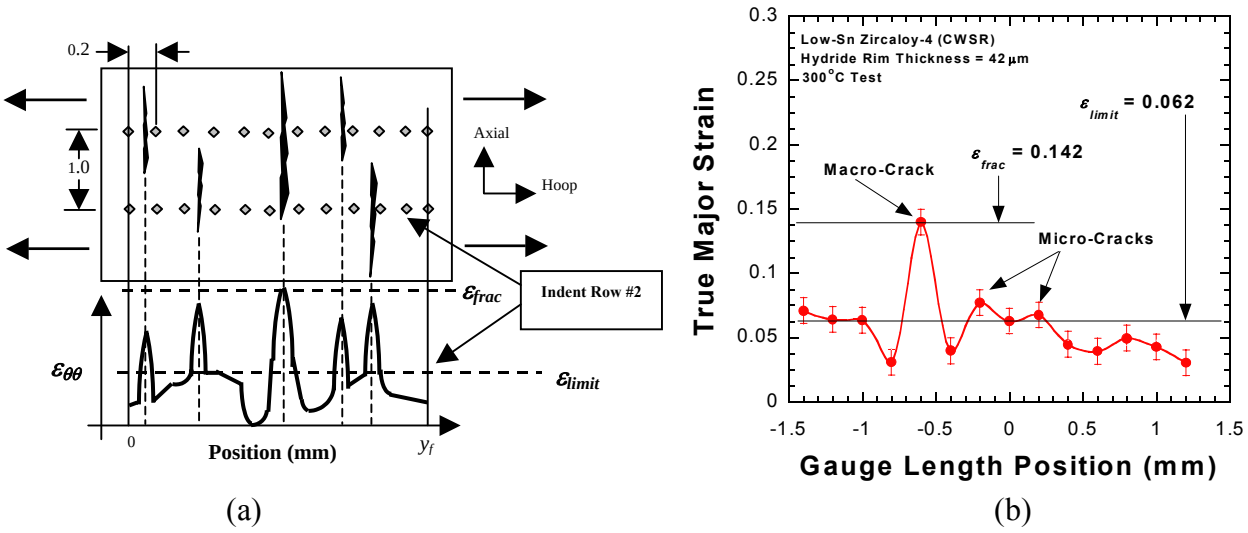

Figure 5 – (a) A schematic of the influence of microcracks on the strain distribution along Indent Row #2 (dimensions in millimeters and not-to-scale) and (b) the measured strain distribution at cladding fracture for a plane-strain ring-stretch specimen with hydride layer thickness of 42 μm tested at 300°C.

As determined on a *local* basis across the fracture surface, the cladding fracture strain, ε_{frac}, is the measure of the local strain required for cladding fracture. Using the procedures described above, we present in Fig. 6 the dependence of both the limit strains (Fig. 6a) and fracture strains (Fig. 6b) on thickness of the hydride layers in Zircaloy cladding tubes deformed to failure at room temperature as well as 300°C *and* under the multi-axial stress state resulting in a near plane-strain. The most important trend in Fig. 6 is the obvious dependence of cladding ductility on hydride-layer thickness. At both room temperature and 300°C, the ε_{limit}-values (Fig. 6a) indicate a gradual ductile-to-brittle transition with increasing hydride layer thickness. Specifically, cladding with hydride rims of thicknesses ≥140 μm show little or no plastic deformation to failure. In view of the fact that the experimental accuracy of our measurements of local strain is ±0.01 (±1%) in strain value, these cladding tubes are essentially brittle. At the 100 μm hydride thickness level, there may be a small level of plastic deformation to the cladding prior to failure. However, cladding samples with hydride-rim thicknesses <90 μm are distinctly ductile with hoop limit strains of roughly 0.04 or greater.

The ductile-to-brittle transition is further defined by considering values of ε_{frac}, as shown in Fig. 6b. Consistent with limit strain behavior, specimens with hydride rim thicknesses ≥85 μm show fracture strains greater 0.1 (10%) while thicknesses >100 μm show <0.05. It is not straight-forward to relate these failure strain values to cladding fracture under an RIA transient. If localization of strain is induced by friction resulting from pellet-cladding interactions, ε_{frac}

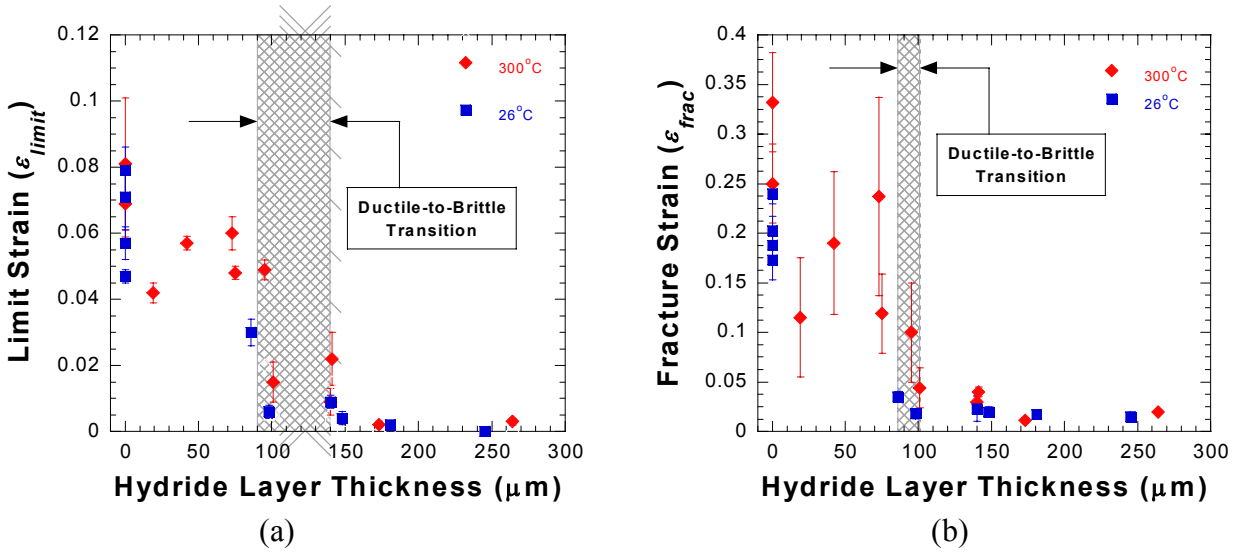

Figure 6: (a) Limit strain (ε_{limit}) and (b) fracture strain (ε_{frac}) as a function of temperature and hydride layer thickness.

may be an important parameters in characterizing cladding failure susceptibility. On the other hand, if fuel pellet-cladding friction is minimal, ε_{limit} may by the more appropriate failure criterion.

It is tempting to consider the results in Fig. 6 on the basis of hydrogen content, as has been done by many previous studies [*8-10,13,14*]. Typically, those studies can identify a significant loss of ductility with increasing hydrogen content such that the factor controlling the ductile-to-brittle transition may be assumed to be the overall hydrogen level. In the present study of Zircaloy tube with a hydride rim, the brittle cladding with *thick* hydride rims had total hydrogen contents ≥500 wppm. However, significant ductility was also observed in specimens with *thin* hydride layers where the cladding had a total hydrogen content ≥700 wppm. Furthermore, our present data indicate cases where cladding in the 500-800 wppm range have similar hydrogen concentrations (but different hydride layer thickness) and fail at widely varying values of ductility. Thus, for the case of a hydride rim, we conclude that the total H level is not the best measure of cladding ductility, but that the ductile-to-brittle transition is better defined by hydride rim thickness. Such a result contrasts the case for uniformly-distributed hydrides across the entire cladding thickness in which the factor controlling the ductile-to-brittle transition is the overall hydrogen level.

Finally, to confirm that the ductility losses presented above in Fig. 6 are indeed caused by the presence of the hydride rim, we present Fig. 7. This figure is based on the behavior of *sibling* specimens with the hydride rim intact and mechanically-removed. These results indicate ductile behavior of cladding, which initially had large hydride rims (173 and 264 μm), *provided* that the rim layer was removed. Removing the hydride rim restores the ε_{limit} and ε_{limit} values to levels close to those determined for non-hydrided cladding.

Summary

We have examined the fracture behavior of Zircaloy-4 cladding tubes containing hydrides precipitated in the form of a hydride rim near the outer surface. Utilizing ring-stretch tests that impose a multi-axial stress state such that near plane-strain tension is achieved in the cladding hoop direction, we conclude the following:

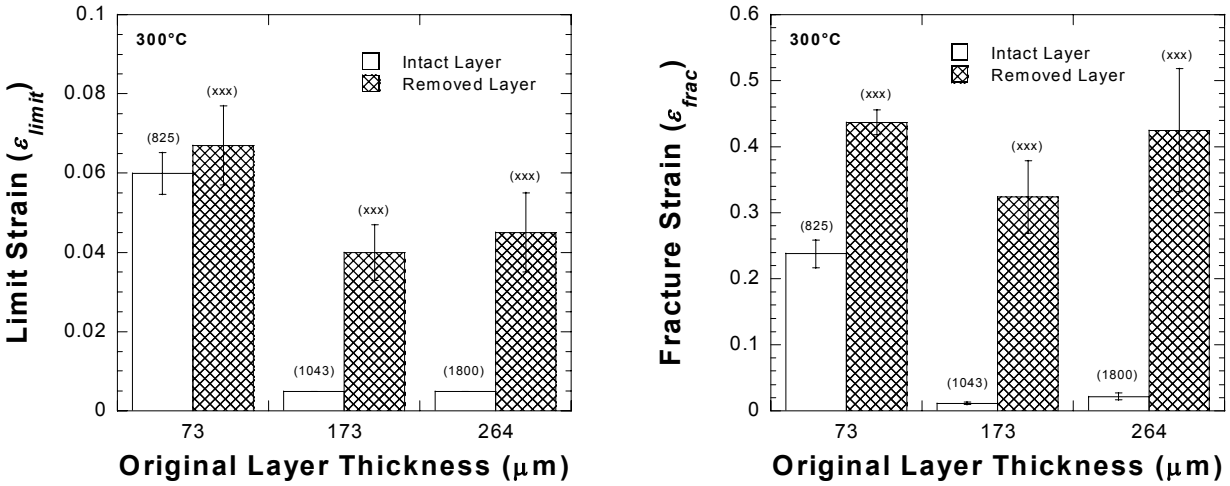

Figure 7: (a) Limit strain (ε_{limit}) and (b) fracture strain (ε_{frac}) as a function of original hydride layer thickness and temperature for cladding with intact layer and removed layer; numbers in parentheses indicate total hydrogen content for specimens.

1. Cladding ductility is very sensitive to hydride-rim thickness at both room temperature and 300°C. This sensitivity is manifested in a loss of ductility with increasing hydride rim thicknesses, such that the cladding is ductile when the hydride rim thickness is less than 90 μm, but it is brittle at hydride rim thicknesses of approximately 140 μm and greater. Our results also indicate that cladding containing <500 wppm total hydrogen remains ductile regardless of whether hydrides are present in the form of a hydride rim or uniformly-distributed hydrides. However, the hydride rim thickness appears to be a more suitable parameter for determining a ductile-to-brittle transition in cladding with a hydride rim.
2. The mechanism of failure of hydrided cladding is identified as multi-stage process involving: (1) microcrack initiation, (2) growth and linkage of microcracks into a long, macrocrack, and (3) failure of the relatively hydride-free ligament by either crack growth due to damage accumulation (room temperature) or the formation of a shear instability beneath a blunted crack (300°C). Since micro-cracks initiate at roughly zero strain, the ductility of cladding at small hydride rim thicknesses appears to be a result of the plastic strain necessary to link micro-cracks into a long surface crack as well as the strain needed to propagate the cracks through the thickness by either damage accumulation or shear instability.

Acknowledgments

We thank Mr. Ozawa, of NDC in Japan, for his preparation of tubing samples with controlled hydride rims. We thank Ross Bradley at Sandvik Metals for supplying the Zircaloy cladding tubes used in this study. The authors would also like to thank Terri Bray, Michael Billone, David McGann and Jakub Dobrzynski of the Irradiation Performance Section at Argonne National Laboratory for technical discussions and experimental assistance. This research was supported by the U.S. Nuclear Regulatory Commission, Office of Nuclear Regulatory Research.

References

1. R.O. Meyer et al., "A Regulatory Assessment of Test Data for Reactivity Initiated Accidents," Nucl. Safety, 37 (1996), 872-387.

2. H.M. Chung, F.L. Yaggee, and T.F. Kassner, "Fracture Behavior and Microstructural Characteristics of Irradiated Cladding," Zr in the Nucl. Ind.: 7th Inter. Sym. (West Conshohocken, PA: ASTM, 1987), 775-801.

3. C. Lemaignan and A.T. Motta, "Zr in Nuclear Applications," Nucl. Mat., 10 (B) (1994), 1-52.

4. J.P. Mardon et al., "Update on the Development of Advanced Zr Alloys for PWR Fuel Rod Claddings," Inter. Top. Mtg. on LWR Fuel Perf. (La Grange Park, IL: ANS, 1997) 405-412.

5. C.E. Ells, "Hydride Precipitates in Zr Alloys," J. of Nucl. Mat., 28 (1968), 129-151.

6. C.E. Coleman and D. Hardie, "The Hydrogen Embrittlement of Alpha Zr-A Review," J. of Less-Com. Met., 2 (1966), 168-185.

7. H.M. Chung et al., "Characteristics of Hydride Precipitation and Reorientation in Spent-Fuel Cladding," Zr in the Nucl. Ind.: 13th Inter. Sym. (West Conshohocken, PA: ASTM, 2002), to be printed.

8. M. Grange, J. Besson, and E. Andrieu, "Anisotropic Behavior and Rupture of Hydrided Zr-4 Sheets," Metall. and Mat. Trans. A, 31A (2000), 679-690.

9. M. Kuroda et al., "Influence of Precipitated Hydride on the Fracture Behavior of Zr Fuel Cladding Tube," J. of Nucl. Sci. and Tech., 37 (8) (2000), 670-675.

10. Y. Fan and D.A. Koss, "The Influence of Multiaxial States of Stress on the Hydrogen Embrittlement of Zr Alloy Sheet," Metall. Trans. A, 16A (1985), 675-681.

11. T.M. Link, D.A. Koss, and A.T. Motta, "Failure of Zr Cladding under Transverse Plane-Strain Deformation," Nucl. Eng. and Des., 186 (1998), 379-394.

12. R.S. Daum et al., "Mechanical Property Testing of Irradiated Zr Cladding Under Reactor Transient Conditions," 4th Inter. Sym. on Small Specimen Test Tech. (West Conshohocken, PA: ASTM, 2002), to be printed.

13. J.B. Bai, C. Prioul, and D. Francois, "Hydride Embrittlement in Zr-4 Plate: Part I," Metall. and Mat. Trans. A, 25A (1994), 1185-1197.

14. P. Bouffioux and N. Rupa, "Impact of Hydrogen on Plasticity and Creep of Unirradiated Zr-4 Cladding Tubes," Zr in the Nucl. Ind.: 12th Inter. Sym. (West Conshohocken, PA: ASTM, 2000), 399-422.

15. T.M. Link, D.A. Koss, and A.T. Motta, "On the Influence of an Embrittled Rim on the Ductility of Zr Cladding," Inter. Top. Mtg. on LWR Fuel Perf. (La Grange Park, IL: ANS, 1997), 634-642.

16. Koji Kitano, private communication with author, JAERI, 26 October 2000.

17. R.S. Daum et al., "On the Embrittlement of Zr-4 Under RIA-Relevant Conditions," Zr in the Nucl. Ind.: 13th Inter. Sym. (West Conshohocken, PA: ASTM, 2002), to be printed.

18. A.M. Garde, G.P. Smith, and R.C. Pirek, "Effects of Hydride Precipitate Localization and Neutron Fluence on the Ductility of Irradiated Zr-4," Zr in the Nucl. Ind.: 11th Inter. Sym. (West Conshohocken, PA: ASTM, 1996), 407-430.

19. T. Fuketa et al., "NSRR/RIA Experiments with High Burnup PWR Fuels," Inter. Top. Mtg. on LWR Fuel Performance (La Grange Park, IL: ANS, 1997), 669-676.